Improved Rotating Kernel Transformation Based Contourlet Domain Image Denoising Framework

Qing Guo[1], Fangmin Dong[1], Shuifa Sun[1,2,*], Xuhong Ren[1], Shiyu Feng[1], and Bruce Zhi Gao[3]

[1] Institute of Intelligent Vision and Image Information, China Three Gorges University, Yichang, 443002, China
[2] Collaborative Innovation Center for Geo-Hazards and Eco-Environment in Three Gorges Area, China Three Gorges University, Yichang, 443002, China
[3] Department of Bioengineering, Clemson University, Clemson, SC, 29634, USA
watersun1977@hotmail.com

Abstract. A contourlet domain image denoising framework based on a novel Improved Rotating Kernel Transformation is proposed, where the difference of subbands in contourlet domain is taken into account. In detail: (1). A novel Improved Rotating Kernel Transformation (IRKT) is proposed to calculate the direction statistic of the image; The validity of the IRKT is verified by the corresponding extracted edge information comparing with the state-of-the-art edge detection algorithm. (2). The direction statistic represents the difference between subbands and is introduced to the threshold function based contourlet domain denoising approaches in the form of weights to get the novel framework. The proposed framework is utilized to improve the contourlet soft-thresholding (CTSoft) and contourlet bivariate-thresholding (CTB) algorithms. The denoising results on the conventional testing images and the Optical Coherence Tomography (OCT) medical images show that the proposed methods improve the existing contourlet based thresholding denoising algorithm, especially for the medical images.

Keywords: Image denoising, Contourlet transform, Direction statistic, Improved Rotating Kernel Transformation.

1 Introduction

The process of image acquisition introduces noise easily, which generates noisy image and have a significant impact on further applications. Lots of useful denoising algorithms have been proposed in past years [1]. In space domain, the denoising methods, such as Lee filter and Rotating Kernel Transformation (RKT) filter, reduce the noise to some extent, but the result is limited [2]. In frequency domain, the denoising algorithm based on wavelet transform has been demonstrated that it can reduce noise

* Corresponding author.

B. Huet et al. (Eds.): PCM 2013, LNCS 8294, pp. 146–157, 2013.

effectively while preserving edges [1]. The literature [3] realizes an efficient retina Optical Coherence Tomography (OCT) image denoising algorithm based on the wavelet transform. In the algorithm, the direction information of the spatial domain is considered by using an artificial setting parameter to control the threshold in vertical subband in wavelet domain. However the algorithm will be invalid while addressing the images of different directions. But its idea is developed further in our work.

Do and Vetterli proposed the contourlet transform to realize the multi-directional and anisotropic representation of image [4]. Since, a series denoising methods based on contourlet transform were proposed. Po and Do [5] proposed the Hidden Markov Tree (HMT) based contourlet denoising method based on the inter-location, inter-scale and inter-direction dependencies of the contourlet coefficients. Guo *.et .al* [6] proposed the bivariate threshold function based contourlet denoising method by taking the inter-direction dependencies into account. Zhou and Shui [7] introduced the local elliptic directional windows to contourlet domain by considering directional information. Nevertheless, this method just modified the shape of window defined by manual operation according to the contourlet transform and ignored the direction information of image. Other more denoising algorithms based on contourlet can be found in [8, 9]. However, the existing contourlet-based threshold denoising algorithms are the extension of the wavelet-based denosing method and their limitations are as follows: 1. in the contourlet transform, the direction information including in space domain is projected into corresponding direction subbands. The noise has no direction and distributes in all subbands uniformly. This will generate the difference between direction subbands. However, the traditional threshold denoising methods don’t consider the difference and build the uniform Probability Distribution Function (PDF) in the Bayes framework, which limits the denoising effect. 2. The contourlet transform has no translation invariance, so the denoising result always contains pseudo-Gibbs effect which has a significant impact on the denoising effect.

In order to solve the first problem, a contourlet transform image denoising framework based on IRKT is proposed. Firstly, an Improved Rotating Kernel Transformation (IRKT) technique is proposed to get the direction statistic and edge information of a given image. The IRKT has the capability of noise immunity, which is discussed by performing experiments. Secondly, the direction statistic reflects the difference between subbands in contourlet domain and is introduced into the threshold function in the form of weights to get a satisfactory denoising result.

2 Relationship between the Image Directions and Subbands of Contourlet Domain

This section demonstrates that the direction information of the given image reflects the valid amount of information included in different direction subbands in corresponding contourlet domain. We perform four scales and eight directions contourlet decomposition to four noisy images containing different direction information shown in Fig.1. (a)-(d), and the results of third scale are showed in Fig.1.(e)-(h). According to the theory of contourlet transform, if a image only contains one kind of direction edge, e.g. Fig.1.(a) which only contains horizontal edge, the main edge information will distribute in the corresponding direction subband after contourlet transform, e.g. Fig1.(e). However, the noise has no direction information and distributes in all of the direction subbands. When the number of direction increases, the direction information will be showed in corresponding the sub-bands, e.g. Fig.1(b)-(d) and Fig.1 (f)-(h). The above phenomenon leads to the different coefficient distribution in different direction subband, as it shown in Fig.1.(e)-(h). The direction information of the given image reflects the valid amount of information included in different direction subbands.

In order to utilize this characteristic, in the denoising algorithm a parameter must be introduced to control the threshold for each direction subband. The subband containing less valid edge information should be processed by a larger threshold to get a better denoising result. According to the experiment showed in Fig.1 (a)-(g), the direction information in the spatial domain can be introduced as the parameter. So, the paper tries to find a novel method to count the directions in a given image and introduces the statistic results into the threshold function in different subbands, this will be discussed in section 3 in detail.

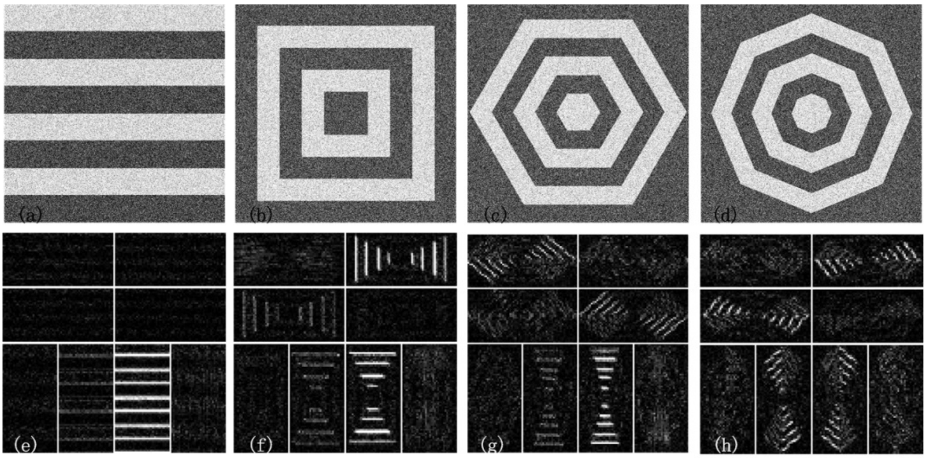

Fig. 1. (a)-(d) are four noisy images containing different number of direction, (e)-(h) are the contourlet decomposition results of (a)-(d)

3 Image Direction Statistic and Weight Model

An Improved Rotating Kernel Transformation (IRKT) is proposed to extract the direction statistic from the given noisy image validly. Various direction kernels are defined to detect the directions of given image. The results of comparing with other conventional edge detection algorithms illustrate that the IRKT can extract the edge information more efficiently, which demonstrate the validity of the direction statistic.

3.1 Improved Rotating Kernel Transformation

Lee and Rhodes proposed the RKT technique which uses several direction kernels to convolve with image and selects the largest convolution of each pixel as the output [10]. Czerwinski *et. al.* use the method to detect the edge of noisy Ultrasound images[11]. Inspired by these works, we propose an Improved Rotating Kernel Transformation (IRKT). The form of kernel is redefined to do better in detecting the edge and counting directions.

Let us define some basic variables. The direction number needing to count is known as *Ndir*; *K* is the size of Kernel, here $K = (Ndir + 2)/2$. In order to explain the process, we make $Ndir = 8$ as the example. The corresponding kernels are shown in Fig.2. I is known as the given image to process. The procedure is as follows:

Step 1: generate the multi direction kernels according to the *Ndir*. Each kernel is defined as k_i (i= 1, 2, … , 8) and shown in Fig.2;

Step 2: execute convolutions to I with ki (i= 1, 2, … , 8) and get eight matrixes Mi (i = 1,2,…,8) which have the same size with I. So each pixel of I known as I(x,y) corresponds eight values $M_i(x,y)$ (i =1,2,…,8) in the eight matrices;

$$M_i = k_i * I \qquad i = 1, 2, ...Ndir \tag{1}$$

Step 3: calculate the standard variation$\sigma(x,y)$ of the eight values $M_i(x,y)$ (i =1,2,…,8). If the$\sigma(x,y)$ is smaller than a threshold T_σ defined in equation (2), the corresponding pixel I(x,y) will be defined as the pixel in the flat area or noise and not be counted, the corresponding eight values $M_i(x,y)$ will be set to zero. The reason for this step is that the pixels of flat areas or noise have no directions and the standard variation of the convolution results of kernels is small. Actually, the procedure defines the edge very well, as shown in equation (3).

$$T_\sigma = \frac{\max(\sigma_p) + \min(\sigma_p)}{2} \tag{2}$$

$$I_{edge}(x, y) = \begin{cases} 1 & \sigma(x, y) > T_\sigma \\ 0 & \sigma(x, y) \le T_\sigma \end{cases} \tag{3}$$

Step 4: select the largest value $Max(x,y)$ among the eight values $M_i(x,y)$ and count the number of selected of i as the frequency of each direction kernel, which generates a 8 dimensional vector known as **Val** and represents the frequency of each direction.

In order to test the validity of this approach, we use the state-of-the-art method, canny and sobel algorithms to detect the edge of four noisy images showed in Fig.1 (a)-(d), and the results are showed in Fig.3.(a)-(l) . The direction statistic results using the proposed method are showed in Fig.3.(m)-(p). The edge detection results indicate that the proposed method can represent edge information more effectively comparing with the canny and sobel algorithm. The statistic results of directions in Fig.3.(m)-(p)

0	1	1	1	1
−1	0	1	1	1
−1	−1	0	1	1
−1	−1	−1	0	1
−1	−1	−1	−1	0

k_1

−1	0	1	1	1
−1	−1	0	1	1
−1	−1	0	1	1
−1	−1	0	1	1
−1	−1	−1	0	1

k_2

−1	−1	0	1	1
−1	−1	0	1	1
−1	−1	0	1	1
−1	−1	0	1	1
−1	−1	0	1	1

k_3

−1	−1	−1	0	1
−1	−1	0	1	1
−1	−1	0	1	1
−1	−1	0	1	1
−1	0	1	1	1

k_4

1	1	1	1	0
1	1	1	0	−1
1	1	0	−1	−1
1	0	−1	−1	−1
0	−1	−1	−1	−1

k_5

1	1	1	1	1
1	1	1	1	0
1	0	0	0	−1
0	−1	−1	−1	−1
−1	−1	−1	−1	−1

k_6

1	1	1	1	1
1	1	1	1	1
0	0	0	0	0
−1	−1	−1	−1	−1
−1	−1	−1	−1	−1

k_7

1	1	1	1	1
0	1	1	1	1
−1	0	0	0	1
−1	−1	−1	−1	0
−1	−1	−1	−1	−1

k_8

Fig. 2. The direction kernels using to count the number of each direction in the image ($NDir = 8$, $K = 5$)

illustrate that the frequency of direction kernels reflect not only the direction information of spatial domain, but also the contourlet decomposition results showed in Fig.1.(e)-(h).

3.2 Direction Weight Model

As the proposed statistic approach can represent the direction information in spatial domain effectively, it is reasonable to use it to build a weight model to represent the valid amount of information in different direction subband. The weight vector is known as $\mathbf{w}_\mathbf{v}$ and defined in equation (4).

$$\mathbf{w}_\mathbf{v}(1, vi) = \frac{\mathbf{Val}(1, vi)}{\sum_{i}^{Ndir} \mathbf{Val}(1, i)} \qquad vi = 1, \dots, Ndir \tag{4}$$

The equation (4) illustrates that the larger the frequency of one direction is, the larger the weight of the direction is. As the relationship between subbands and direction information in the contour domain illustrated in section 2, the weight can be explained as: the more the valid amount of information of one direction sub-band contains, the larger the weight of the direction is. So it’s reasonable to use the weight vector to control the threshold of direction subbands by considering the different valid information in direction subbands.

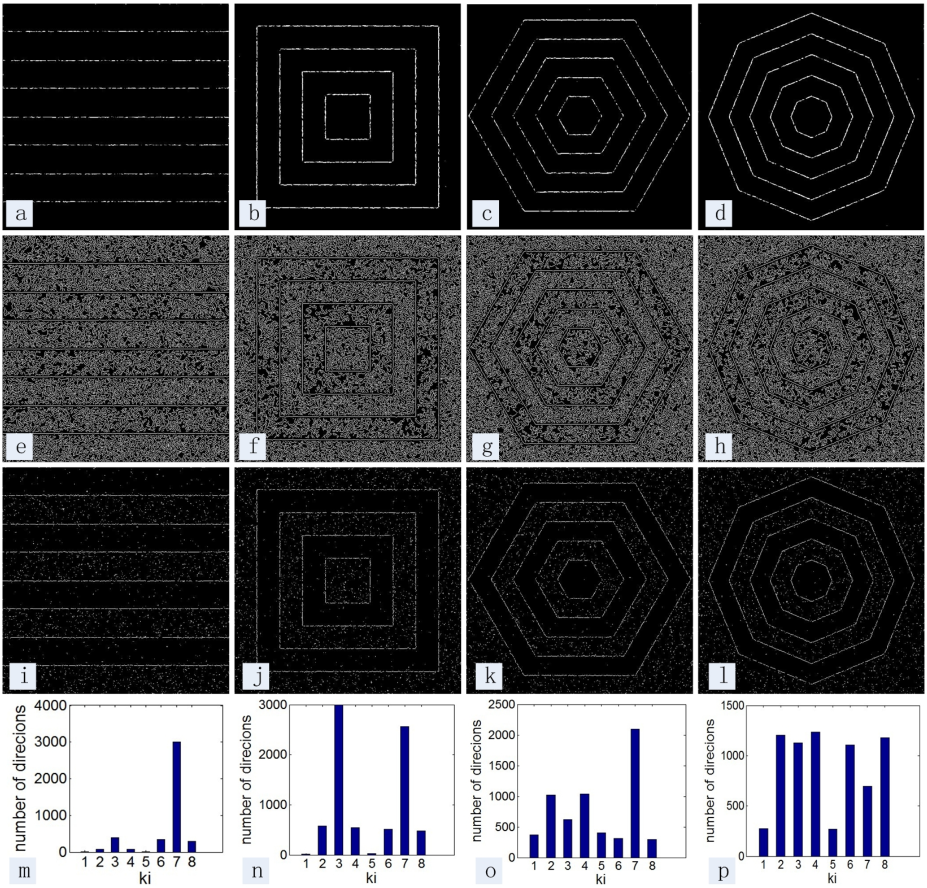

Fig. 3. (a)-(d), (e)-(h), (i)-(l) the edge detection results of the noisy images in Fig.1 by using IRKT, canny and sobel, respectively; (m)-(p) the directions frequency statistic of (a)-(d)

4 Novel Contourlet Transform Denoising Framework Based on IRKT

The basic threshold denoising method for contourlet transform is to deduce a shrinkage function, such as hard threshold function, soft threshold function, bivariate shrinkage function and so on, to handle every coefficient in the transform domain and get the approximation of noiseless coefficients. Then the denoised image can be gotten by contourlet inverse transform. The key of this process is to build an efficient shrinkage function. However, the traditional method only focuses on the characteristic of each direction subband itself, and the difference between subbands is ignored, so the denoising effect is limited.

According to the above introduction, the paper proposes a novel threshold denoising framework for contourlet transform based on IRKT. The process is illustrated as follow and showed in Fig.4 . This framework is used to improve the soft threshold and bivariate threshold denoising method base on contourlet transform. Here, the improved soft and bivariate threshold algorithms based on contourlet transform are labeled as CTSoftDB and CTBDB, respectively.

Step1: perform contourlet transform to the noisy image *I*. *I* can be defined as equation (5).

$$Y=X+N \tag{5}$$

Where Y is noisy image, X is the noiseless pixel, N is the additive noise. The transform result is:

$$y_{i,j} = w_{i,j} + \varepsilon_{i,j} \tag{6}$$

Where y , w and ε is the corresponding noisy coefficient, noiseless coefficient and noise coefficient in contourlet domain, respectively .Here we assume ε is the gaussian noise. j, i represents the decomposition level and the direction subband being discussed, respectively.

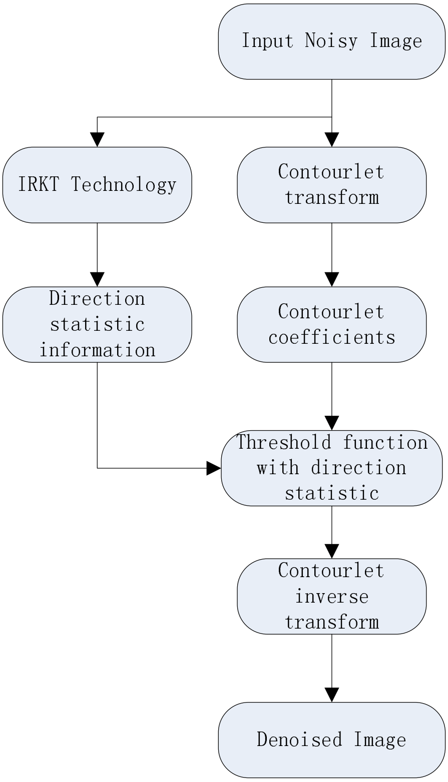

Fig. 4. The proposed threshold denoising framework

Step2: in the decomposition level j, the number of direction sub-bands is $Ndir_j$. Use the method proposed in section 3 to get the direction weight $\mathbf{w_{v,j}}$ of the image in spatial domain with the input $Ndir_j$.

Step3: get the shrinkage function $T(y)$ according to different method mentioned in [4, 6].

Step4: use equation (7) to handle each coefficient in the decomposition level j and direction subband i, and do the same to other subbands and decomposition levels.

$$\hat{\omega}_{i,j} = \left(\frac{c}{\mathbf{w_{v,j}}(1,i)+1}\right)\cdot T(y_{i,j}) \tag{7}$$

where $\hat{\omega}_{i,j}$ is the evaluation of the noiseless coefficient, c is a constant to control the extent of the weight.

Step5: perform contourlet inverse transform to the denoised contourlet coefficients and get the denoised image.

5 Experiments

In this section, several conventional testing images and Optical Coherence Tomography(OCT) images are regarded as test images to compare the Wavelet threshold denoising algorithm based on bivariate function (WTB)[12], Contourlet soft threshold denoising algorithm(CTSoft)[4], Contourlet bivariate threshold denoising algorithm (CTB) [6] and two proposed denoising methods (CTSoftDE and CTBDE). The denoising results including metric values illustrate that the proposed denoising framework improves the existing methods. The parameter c in (7) is set to 1.3 for all experiments.

5.1 Metrics

For the standard test images, since the noiseless images are given, the Peak Signal to Noise Ratio (PSNR) and $\beta$are adopted to evaluate the denoising effect and the edge preserving effect [3], respectively. For OCT images, the metrics Signal to Noise Ratio(SNR), Contrast to Noise Ratio (CNR) and Equivalent Number of Look (ENL) are used to evaluate the denoising result[2, 3].

5.2 Experiments and Analysis

Experiment A. conventional testing images denosing experiment

Five algorithms are used to denoise four standard test images showed in Fig.5 (img1-img4). The testing images are added additive gaussian noise with the variance of 0.02 and mean of 0. PSNR and $\beta$are regarded as the metrics to evaluate the denoising results and showed in Table.1. The detected edges are showed in Fig.5.(b).

The denoising results of CTSoftDE and CTBDE are shown in Fig.5.(c) and (d). The experiment indicates that the proposed methods do better in improving the image quality. However the edge information loses to some extent. The reason is that the nature images contain abundant texture information. As a result, the subbands of contourlet domain will also contain amount of texture information, and the uniform lifting threshold will lead to lose some edge information. However, most of the medical images do not have much more detail texture and may mainly contain one direction information. In this case, the proposed framework will do better, as it showed in the B experiment.

Experiment B. OCT Images denoising experiment

In order to test the validity and application of the proposed method, five low SNR OCT images are denoised by using different algorithms. Actually, according to the experiment B, this kind of medical images does not contain the detail texture, so the proposed algorithms will do better. The method proposed in [13] is used to estimate the noise level of the OCT images. The denoising results of five algorithms are shown in Fig.6 and Table.2. The value in the table represents the mean of the selected ROI. The results indicate that the proposed method improves the SNR of the test images, and the CTBDE algorithm based on bivariate threshold function does better than the CTSoftDE for taking the dependency of contourlet coefficients in different scales into account. The CNR has also been improved. The increasing of ENL illustrates that the proposed method smoothes the flat area.

Table 1. PSNR and βvalue of the denoised images in Fig.5

		Noisy	WTB	CTSoft	CTB	CTSoft DE	CTBDE
Img1	PSNR	17.18	26.09	26.45	26.62	26.60	26.65
	β	0.22	0.19	0.29	0.29	0.29	0.28
Img2	PSNR	17.17	26.58	26.50	26.78	26.69	26.89
	β	0.13	0.13	0.17	0. 17	0.16	0.16
Img3	PSNR	17.26	25.68	25.92	26.05	26.07	26.11
	β	0.21	0.17	0.27	0.26	0.26	0.26
Img4	PSNR	17.14	24.86	25.45	25.58	25.56	25.62
	β	0.32	0.18	0.37	0.37	0.38	0.36

Fig. 5. The denoising results of proposed method. Row 1 to 4 is the Img2 to 4, respectively. Column (a) are the noisy images. Column (b) are the dected edges by using the IRKT. Column (c) and (d) are the denoising results of CTSoftDE and CTBDE.

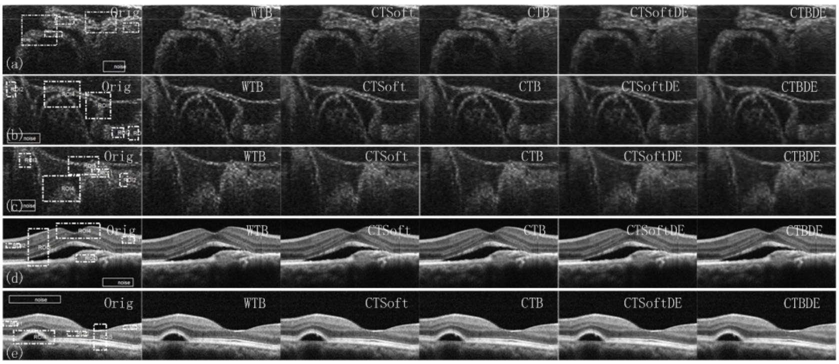

Fig. 6. (a)-(e) are the denoised OCT images based on five algorithms. The first column is the original noisy images, the algorithm used is showed on the top right corner. The images (d) and (c) come from the http://www.optos.com/en/Professionals/Image-library/

Table 2. SNR, CNR and ENL of the denoised images in Fig.6

		Orig	WTB	CTSoft	CTB	CTSoft DE	CTBDE
OCT1	SNR(dB)	17.78	19.72	19.93	20.14	20.85	21.37
	CNR	5.67	6.17	6.21	6.29	6.45	6.61
	ENL	6.47	10.79	14.63	15.74	20.90	25.27
OCT2	SNR(dB)	16.06	18.31	18.46	18.54	19.56	20.18
	CNR	4.42	4.96	5.01	5.08	5.30	5.45
	ENL	7.08	11.889	16.16	17.33	21.10	24.05
OCT3	SNR(dB)	18.97	20.95	21.36	21.69	22.54	23.02
	CNR	6.11	6.50	6.56	6.58	6.74	6.81
	ENL	8. 50	14.93	17.53	19.65	23.98	24.93
OCT4	SNR(dB)	24.08	24.65	24.93	25.06	25.51	25.63
	CNR	8.88	9.13	9.18	9.22	9.33	9.37
	ENL	37.96	56.19	56.31	58.36	61.50	64.71
OCT5	SNR(dB)	21.70	22.13	22.31	22.45	22.75	22.94
	CNR	8.77	9.04	9.09	9.12	9.24	9.33
	ENL	36.95	62.41	64.37	65.97	72.10	75.03

6 Conclusion and Prospect

A novel contourlet transform denoising framework based on IRKT is proposed. The IRKT method is proposed to get the direction statistic representing the difference between subbands and edge information. The direction statistic is added to the existing shrinkage functions. As a result, a novel denoising framework is gotten and used to the soft and bivariate thresholding methods. The experiment results indicate that the proposed methods reduce the noise and improve the SNR efficiently, especially for the medical images, e.g. OCT images. Actually, the paper proposes a novel thresholding denoising framework instead of a novel threshold function to achieve a general improvement of various thresholding denoising methods based on contourlet transform, which may be extent to the denosing methods based on other transformation tools in the future. On the other hand, the edge information exacted in section 3 is not used. The future work will focus on completing the edge exacting process and its use in denoising framework.

Acknowledgements. This project is supported by National Natural Science Foundation of China (61102155, 61272237, 61272236), Outstanding Young and Middle-aged Innovative Research Team Plan of Hubei Province of China (T201002), the Graduate students scientific research innovation fund of the China Three Gorges University(2012CX044), the Graduate students excellent academic dissertation fund of the China Three Gorges University(2013PY038).

References

1. Buades, A., Coll, B., Morel, J.M.: Image Denoising Methods. A New Nonlocal Principle. SIAM Rev. 52(1), 113–147 (2010)
2. Aleksandra, P., Ljubomir, J., Bruno, H., Vladimir, Z., Paul, D., Frans, D., Wilfried, P.: Multiresolution denoising for optical coherence tomography: a review and evaluation. Curr. Med. Imaging Rev. 4(4), 270–284 (2010)
3. Adler, D.C., Ko, T.H., Fujimoto, J.G.: Speckle reduction in optical coherence tomography images by use of a spatially adaptive wavelet filter. Opt. Lett. 29(24), 2878–2880 (2004)
4. Do, M.N., Vetterli, M.: The contourlet transform: a efficient directional multiresolution image representation. IEEE Trans. Image Process. 14(12), 2091–2106 (2005)
5. Po, D.D.Y., Do, M.N.: Directional Multiscale Modeling of Images using the Contourlet Transform. IEEE Trans. Image Process. 6(15), 1610–1620 (2006)
6. Qing, G., Fangmin, D., Shuifa, S., Bangjun, L., Zhi, G.: A Novel Image Denosing Algorithm Based on Contourlet Transform for Optical Coherence Tomography Heart Tube Image. IET Image Process (to be appeared)
7. Zhou, Z.F., Shui, P.L.: Contourlet-based image denoising algorithm using directional windows. Electron. Lett. 43(2), 92–93 (2007)
8. Godzwon, M., Saeed, K.: Biometrics Image Denoising Algorithm Based on Contourlet Transform. In: Bolc, L., Tadeusiewicz, R., Chmielewski, L.J., Wojciechowski, K. (eds.) ICCVG 2012. LNCS, vol. 7594, pp. 735–742. Springer, Heidelberg (2012)
9. Tian, X., Jiao, L., Zhang, X.: Despeckling SAR images based on a new probabilistic model in nonsubsampled contourlet transform domain. Signal Image Video P. (2012), doi:10.1007/s11760-012-0379-0
10. Lee, Y.K., Rhodes, W.T.: Nonlinear image processing by a rotating kernel transformation. Opt. Lett. 15(23), 1383–1385 (1990)
11. Czerwinski, R.N., Jones, D.L., O'Brien, W.D.: Detection of lines and boundaries in speckle images-Application to medical ultrasound. IEEE Med. Imag. 18(2), 126–136 (1999)
12. Sendur, L., Selesnick, I.W.: Bivariate shrinkage functions for wavelet-based denoising exploiting inter-scale dependency. IEEE Trans. Signal Process. 50(11), 2744–2756 (2002)
13. Donoho, D.L., Johnstone, I.M.: Ideal spatial adaptation by wavelet shrinkage. Biometrika 81, 425–455 (1994)